

International Space Station Assembly and Operation Control Challenges

Nazareth S. Bedrossian

© AAS. Reprinted, with permission, from the 23rd Guidance and Control Conference held in Breckenridge, CO, February 3-6, 2000, and was originally published in the AAS publication "Guidance and Control 2000" Advances in the Astronautical Sciences



ABSTRACT

For the International Space Station (ISS) program to be successful, mission requirements must be met robustly in the presence of uncertainties. Changing Station characteristics during assembly, such as variability in structural flexibility and mass properties, pose unique control challenges. Three examples of control challenges are reviewed in this paper; the first two arise out of variability in flex structure, and the last one is due to mass property variation. Controller/flex structure interaction issues and their origins are reviewed as well as representative examples. Control moment gyroscope (CMG) momentum desaturation issues during robotic operations are addressed, and an operational solution is reviewed. Finally, CMG attitude control issues during robotic payload operations are presented, as well as an issue resolution technique.

INTRODUCTION

The assembly and operation of the Space Station pose unique control challenges due to its complex, variable flexible structure and mass properties during assembly, as well as the variety of operational modes and control systems. Operational modes include attitude control for mated and unmated configurations, reboost, and robotic payload operations. For the program to be successful, mission requirements must be met using a variety of control systems from various International Partners. These include the Russian propulsive attitude control systems (ACS) on the functional cargo bay (FCB) cargo block, service module (SM) and Progress resupply vehicle, the U.S. CMG nonpropulsive ACS and the U.S. propulsive options using the interim control module (ICM) and propulsive module (PM), the Canadian Space Station Remote Manipulator System (SSRMS), as well as the mobile transporter (MT), etc. An overview of the various Space Station elements supplied by the participating International Partners is shown in Figure 1. Further, these attitude control systems must be robust to system uncertainties and variations in flex structure, mass properties, failures, and initial conditions. Hence, it

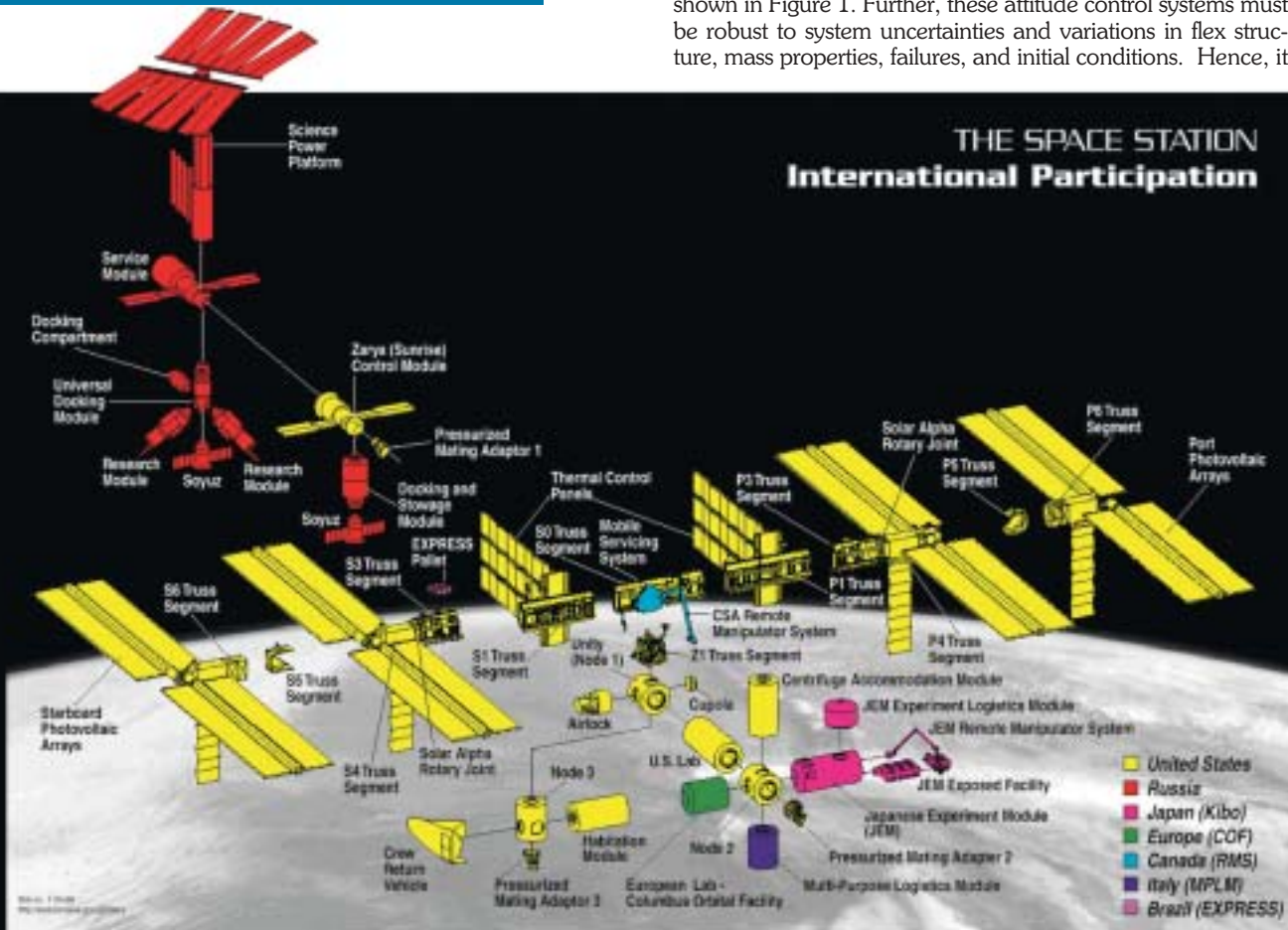


Figure 1. International Space Station – Partner Nations and Elements.



is critically important that an integrated system assessment of the guidance, navigation, and control (GN&C) system robust stability and performance be carried out in order to certify the vehicle for flight readiness.

Of paramount importance is avoiding control system/flex structure interaction or dynamic interaction, especially when the Station is under propulsive attitude control. These feedback instabilities or resonances can compromise the structural integrity and lifetime of the vehicle due to large induced peak and fatigue loads and by using excessive propellant. This may result in planned operations having to be postponed or cancelled. The integrated control system flex structure assessment and flight readiness certification process must identify the potential for dynamic interaction, and if necessary, develop operational workarounds. For the early stages, where flex dynamics are dominant, flex filter architecture and coefficients have to be tailored carefully to preclude the possibility of the attitude control system responding in phase with these resonances.

Attitude control during robotic payload operations poses a particularly challenging issue. In general, robotic arm flexibility is large and low enough in frequency to be inside the attitude controller bandwidth. This is a particular issue especially during attitude maneuvers, which can and usually do excite robot arm flexibility. Another robotic flex issue is the impact of open-loop thruster firings during Station momentum desaturation. In this case, the issue is peak-induced structural loads that impact the operational lifetime of the arm. Hence, the desaturation firings must be performed in a manner that does not compromise the structural integrity of the arm. Another issue with robotic payload operations is the resulting variability in mass properties and their impact on CMG attitude control. The issue in this case is CMG momentum and torque saturation. This situation is undesirable because it impacts the operational timeline and also requires the use of attitude control thrusters to desaturate the CMGs.

This paper addresses control challenges related to the assembly and operation of the ISS. Changing Station characteristics during assembly, such as variability in structural flexibility and mass properties, pose control challenges that must be addressed for a successful Station program. Three examples of control challenges are reviewed in this paper; the first two arise out of variability in flex structure, and the last one is due to mass property variation during robotic assembly operations. Controller/flex structure interaction issues and their origins are reviewed, as well as representative examples for a particular assembly stage. CMG momentum desaturation issues during robotic operations are addressed, and an operational solution to induced structural loads is reviewed. Finally, CMG attitude control issues during payload robotic operations are presented, as well as an issue resolution technique using a momentum optimal CMG maneuver logic.

Control System Flex Structure Interaction

A basic requirement for any space vehicle is that its control systems are stable and meet performance specifications in the presence of uncertainties. For the Space Station attitude control system to be stable, avoiding control system/flex structure interaction (CSI) or dynamic interaction is necessary.

Dynamic interaction is most likely when the Station is under propulsive attitude control due to the large control authority of the reaction control system (RCS). The standard definition of dynamic interaction is that of feedback control instability. For phase-plane controlled systems such as the Station, this implies a growing limit cycle. These feedback instabilities can result in large peak and fatigue structural loads, as well as use excessive propellant. Such a situation may result in planned operations being postponed or cancelled. The cause of feedback instabilities is prolonged flex-induced firings that reinforce structural flex, i.e., the thruster firings do not damp flex, but rather add energy to the system. The cause for this phenomenon is in-phase, with respect to flex, thruster firing. However, even persistent high-frequency limit cycles are classified as instabilities as they lead to an unacceptably high rate of propellant use. In general, for phase-plane-based attitude control systems, inadequate control system attenuation and excessive lag are the cause for dynamic interaction.

The integrated control system assessment and flight readiness certification process must identify the potential for dynamic interaction and, if necessary, develop operational workarounds. For the early Space Station stages, where flex dynamics are dominant, flex filter architecture and coefficients have to be tailored carefully to preclude the possibility of the attitude control system responding in phase with these resonances.

Space Station Structural Flexibility Overview

During the assembly and operation of the Space Station, the complex and varying flexible structure provides one of the necessary ingredients for potentially undesirable or even unstable CSI. The main cause is low-frequency and large-amplitude flexibility, due primarily to articulating solar arrays, but can also be caused by robotic arm flexibility. Further, as the assembly progresses from early nearly symmetrical stages to late stage complex configurations, the structural frequency spectrum exhibits progressively more complex characteristics, such as densely packed modes, lower frequency modes, and directionally coupled dominant modes.

A brief overview of structural flexibility during assembly is shown in Figures 2 through 5. Each of these figures shows a particular stage in the Station assembly sequence, a frequency response plot (singular value decomposition) from thruster commands in roll, pitch, and yaw to the rate gyro sensor (in deg/s), and the input/output directional decomposition (singular directions) for the three highest amplitude flex modes. Figure 2 shows the characteristics for Stage 1R, which is currently the next stage in the assembly sequence. Stage 1R is formed when the Russian service module vehicle docks to the FGB module already in orbit. Figure 3 depicts Stage 4A during robotic assembly using the SRMS with payload, the first U.S. solar arrays. Figure 4 shows the completed assembly for Stage 4A, and Figure 5 provides detail on Stage 13A. From the figures it is evident that 1R has two dominant roll and the largest amplitude modes, 4A+robotics has very low-frequency dominant modes that are lower than the lowest Station structural mode, while 4A and 13A show modes in lower frequencies with higher density.



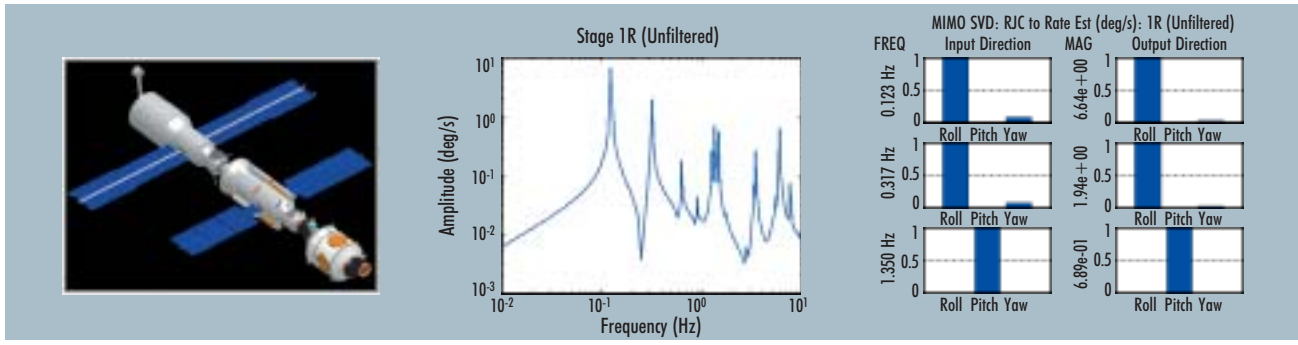


Figure 2. Stage 1R: configuration, frequency, and directional response.

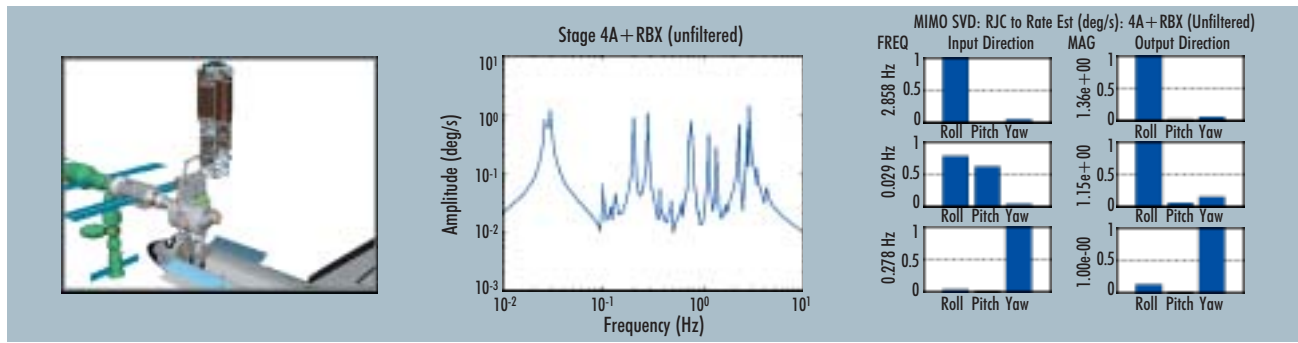


Figure 3. Stage 4A+Robotics: configuration, frequency, and directional response.

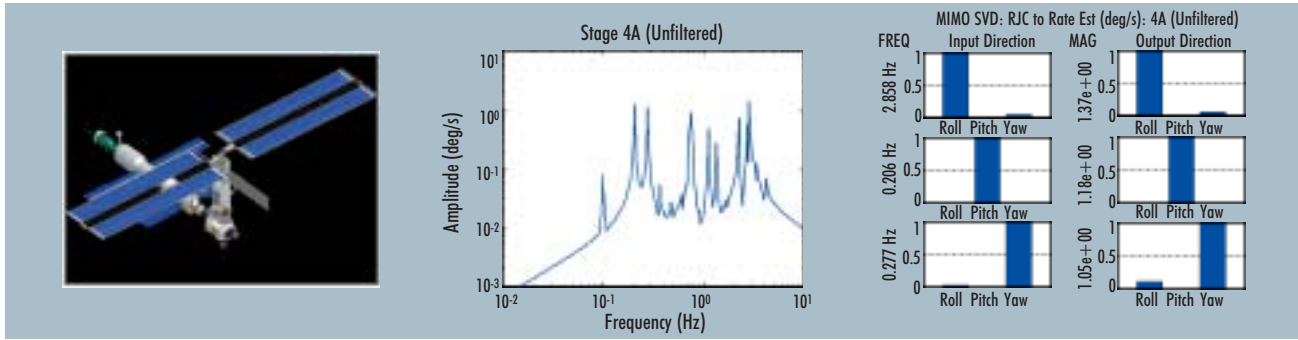


Figure 4. Stage 4A: configuration, frequency, and directional response.

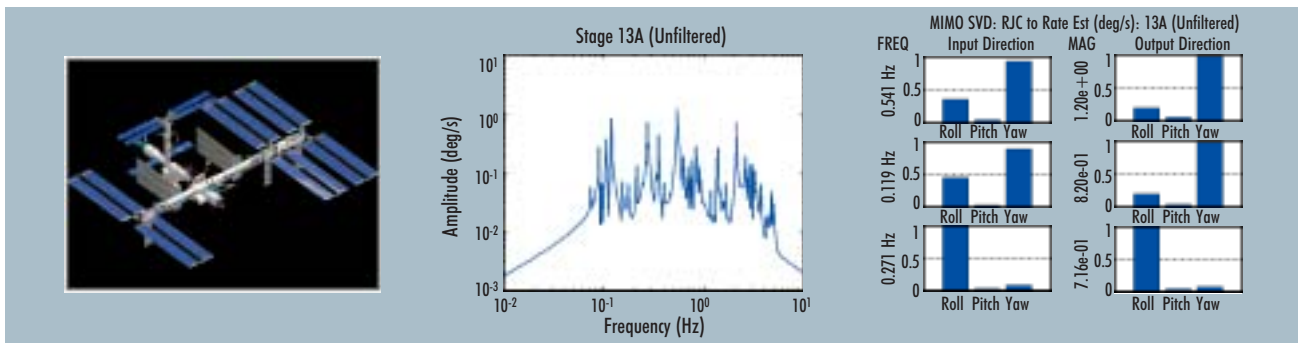


Figure 5. Stage 13A: configuration, frequency, and directional response.



A further complication in the Station structural flexibility is the issue of uncertainty. The flex models and their characteristics discussed in the previous paragraph are based on finite-element models. Based on test results and estimates made, flex model uncertainty levels have been established for flex body robustness analyses and flight parameter verification: modal damping ratio of 0.5%, an uncertainty in modal frequency of $\pm 20\%$, and an uncertainty in mode shape of $\pm 50\%$. The uncertainty in the mode shape results in a peak amplitude uncertainty of 125%. Further, given the uncertain nature of integrating U.S. and Russian hardware and models and taking into consideration the uncertainties used by the Shuttle Program Office for Shuttle mated structural models,^[1] the uncertainty in frequency can be prudently expanded to $\pm 30\%$.

Space Station Propulsive Flight Control System Overview

The ISS propulsive attitude control system provides rotational and orbital velocity control. The propulsion capabilities of the ISS reside entirely within the Russian segment on three separate vehicles: the FGB, the SM, and the Progress resupply vehicle. However, for the majority of the Space Station's lifetime, the SM will provide the propulsive flight control function and will be used in this paper to illustrate the CSI problem. The SM motion control system (MCS) provides all the algorithms for control of the Station, including flex rate filters, maneuver logic, phase-plane control law, reboost control law, thruster restriction logic, and jet select. The MCS algorithms assume only control of the rigid-body attitude and rate, thus requiring attenuation of any flexible dynamics.

The flex rate filters are used to provide an estimate of the rigid-body rate for use in the phase-plane control law. An overview of the filter architecture is shown in Figure 6. A second-order, low-pass ~ 0.05 -Hz bandwidth filter in each axis is used to attenuate low-energy, high-frequency bending modes and to minimize the effects of sensor noise and quantization. In estimating the rigid body vehicle rate, the flex filters rely on feedforward prediction of the jet firing rate change to account for the slow 5-Hz sensor update rate and to allow the use of a low-bandwidth, low-pass filter, i.e., the filter is only required to filter the error in the prediction of the jet firings and not the entire rate change. Additionally, a disturbance filter is also used to estimate slowly-varying unmodeled disturbances. To attenuate low-frequency bending modes that may not be attenuated adequately by the low-pass filter, a series of three second-order notch filters per axis are also used. The algorithms also provide adaptive tuning of the notch frequencies during flight to account for uncertainties in the structural model. The frequency response of the flex filter from measured rate input to estimated rate output is shown in Figure 7. Note that the notch locations in Figure 7 have been selected purposely in order to illustrate the CSI example that follows.

CSI Example – Stage 1R

In this section, examples of unstable CSI are presented for assembly stage 1R, and the causes of the interaction are identified. Given the nonlinear nature of phase-plane control laws in general, standard stability techniques are difficult if not impossible to apply. A linear phase plane equivalent cannot be

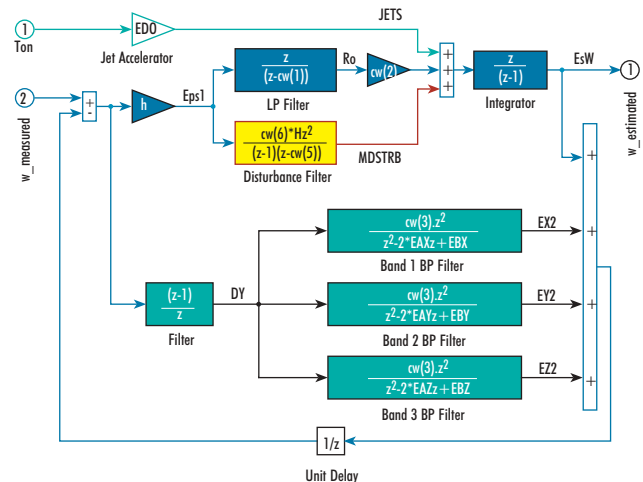


Figure 6. Russian SM MCS – flex filter architecture.

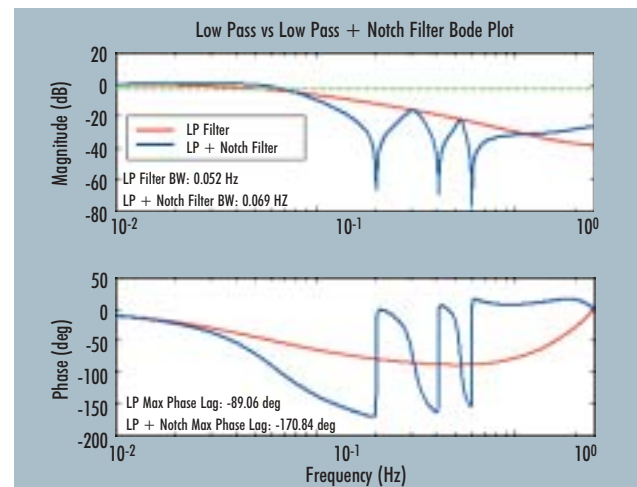


Figure 7. Russian SM MCS – flex filter frequency response.

developed that represents the nonlinear controller adequately, and standard nonlinear analysis techniques, e.g., describing function analysis, have been shown to be so conservative as to return unusable results.^[2]

In general, for switching control systems such as phase planes, the typical CSI occurs when filtered flex oscillations are large enough to exceed both positive or negative rate deadbands. In an idealized situation, with the rigid rate estimate centered between the switch curves (assuming symmetric rate deadbands), rate-to-rate deadband exceedance results in bipolar firings. Some of the causes of this phenomenon are insufficient attenuation of flex dynamics in the rate estimate, very small rate deadbands, very high jet thrust, high-frequency jet firings, and excessive phase lag. Therefore, if the filtered rate estimate does not exceed the rate deadband, a dynamic interaction cannot be induced, hence, an unstable dynamic interaction cannot occur. Under appropriate assumptions, filtered flex amplitude less than the rate



deadband provides a sufficient condition for flex stability. However, if the rate deadband is exceeded, it is not necessary that an unstable dynamic interaction develop. One condition that can lead to instability is sufficient phase lag such that the deadband exceedence-induced firings are in phase with the structural (unfiltered) flex dynamics. However, even then, a rate-to-rate deadband oscillation may not result unless jet thrust is large or frequent. Note that the phase lag applies to the transfer function from the actuator node to the phase plane input. An example for Stage 1R flex structure is shown in Figure 8, which represents the transfer function from three-axis jet command to rate sensor. The phase lag for the dominant mode at 0.12 Hz is nearly zero, 0.4 deg. For the transfer function just described and using appropriate assumptions, 90 deg is sufficient phase lag to cause in-phase thruster firings. Hence, one of the necessary conditions for instability is that phase lag exceeds 90 deg.

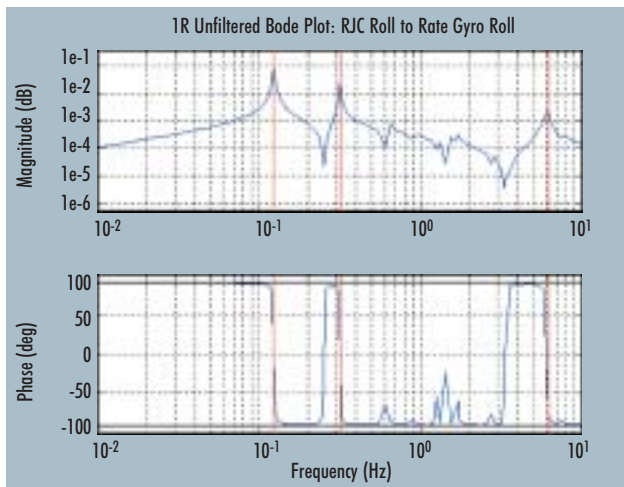


Figure 8. Stage 1R flex model roll axis magnitude and phase response.

Due to the nonlinear nature of the phase-plane control system, predicting instances of unstable dynamic interaction can be challenging. An example of the type of radically different responses that can be obtained due to small changes in maneuver angle is shown in Figure 9, a CSI instability, and Figure 10, which shows a stable CSI example. The example configuration is Stage 1R where the flex frequencies have not been perturbed, while the peak flex amplitude has been increased by 100%. The commanded maneuver rate in both cases is 0.2 deg/s. Figure 9 depicts the results for an 18.65-deg roll maneuver, while Figure 10 shows the results for a 19.2-deg maneuver. The flex filter notches for both examples are initialized as shown in Figure 7, i.e., the first roll notch is initialized purposely at 0.2 Hz, while the roll-dominant mode is at ~0.12 Hz. In a real-world situation, the dominant flex modes will not be known precisely, hence, without in-flight system identification or adaptation, the discrepancy between notch and dominant mode could be large. This example shows the severe repercussions that may result.

From Figure 9, it is evident from the phase-plane plot that rate deadband to rate deadband flex oscillations are observed. The jet firings are in phase with the measured structural modes, as can be seen from the measured vs jet on-time plots. This is an example of an unstable dynamic interaction.

It is caused by the secondary rigid body rate damping firings that occur when the attitude error is 15 deg, as indicated on the phase plane. This behavior is a feature of the SM MCS phase plane. Rate damping is used to decelerate the vehicle during the terminal phase of the maneuver. This firing, which occurs at ~20 s, is sufficiently large and in-phase with the structural mode at 0.12 Hz, thus exciting the mode sufficiently that rate-to-rate deadband flex oscillations result. It may be noted that the rate damping firings are a function of the 15-deg transition zone rate estimate. From the phase-plane plot, the rate error is positive, indicating that the actual maneuver rate at the instant of transition is actually greater than the commanded rate. This is the cause for the large rate damping firing.

Comparing the results in Figure 10 with those in Figure 9, it is clear that the results in Figure 10 indicate a stable dynamic interaction. In this case, the rigid-body rate damping firing at 15 deg or ~25 s is out of phase with the structural flex, thus attenuating flexure. Even though the flex filter phase lag exceeds 90 deg at 0.12 Hz, the CSI is stable because the flex-induced firings are not large enough to excite rate-to-rate deadband flex oscillations. Further, the rate damping firings are substantially smaller in this case. From the phase-plane plot, the rate error is negative, indicating that the actual maneuver rate at the instant of transition is actually smaller than the commanded rate. This is the cause for the smaller rate damping firing.

CMG Momentum Desaturation

During assembly of the ISS, robotic manipulation of various payloads will be required. The SRMS and the SSRMS will manipulate the payloads. During these assembly operations, attitude control is provided primarily by the U.S. CMG system. Since the angular momentum of the CMG system is limited, manipulating relatively heavy payloads may cause large momentum transients, resulting in momentum and torque saturation. Hence, momentum desaturation requires the use of thrusters.

Thruster activity during robotic payload operations poses certain subsystem-specific issues. The primary issue is excessive robotic structural loads due to either large or periodic thruster firing. The desaturation-induced firings should avoid exciting the robotic arm to its load limits, and must also be robust to variable arm dynamics. Further, frequent desaturations are undesirable as they increase operational complexities and the time required to complete the robotic operation. The implementation should also be compact with respect to onboard computer memory use. Also, limited desaturation times are desirable in order to minimize impact to operational timelines. To reduce program costs both in design and verification phases, a single approach is to be used for all Station assembly stages and robotic operations. Finally, the desaturation must also be flexible so that the technique used to satisfy robotic structural loads does not hinder the ability to remove momentum during docking operations. In the following sections, the CMG momentum desaturation method developed by Draper Laboratory for the ISS for use during robotic payload operations is reviewed.

Thruster momentum desaturation can be accomplished in a variety of ways. It can be classified as either closed loop (feedback) or open loop (feedforward). For closed-loop methods,



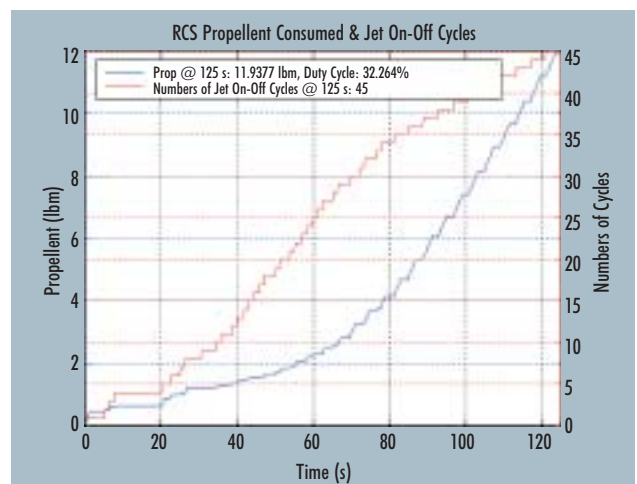
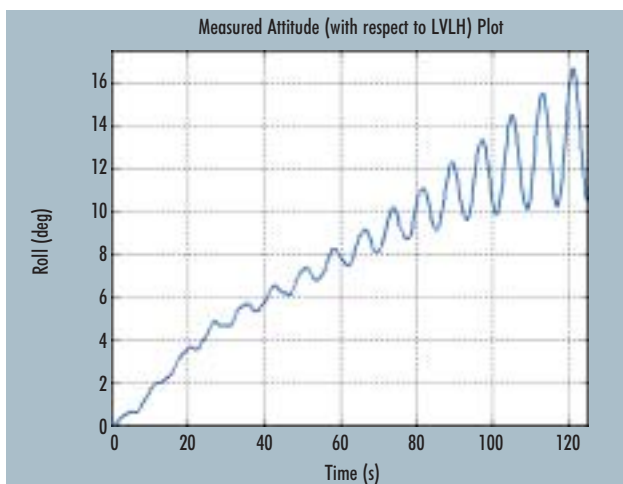
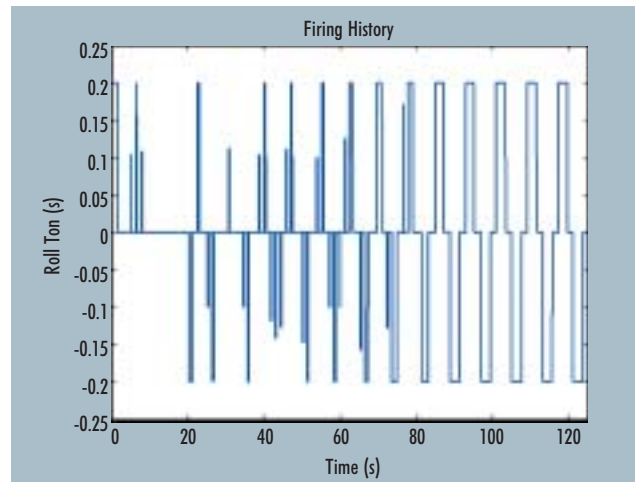
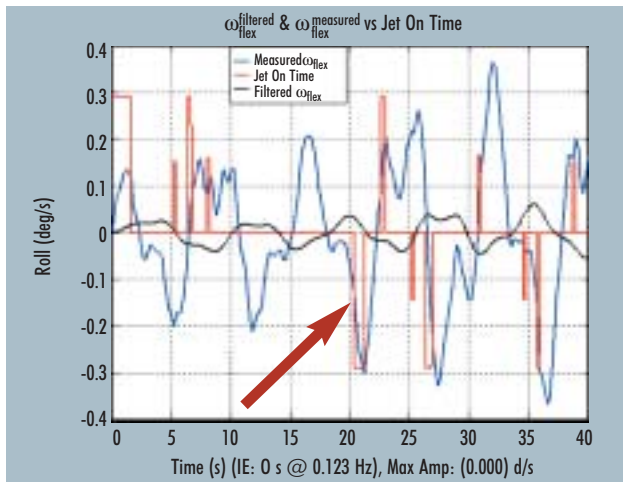
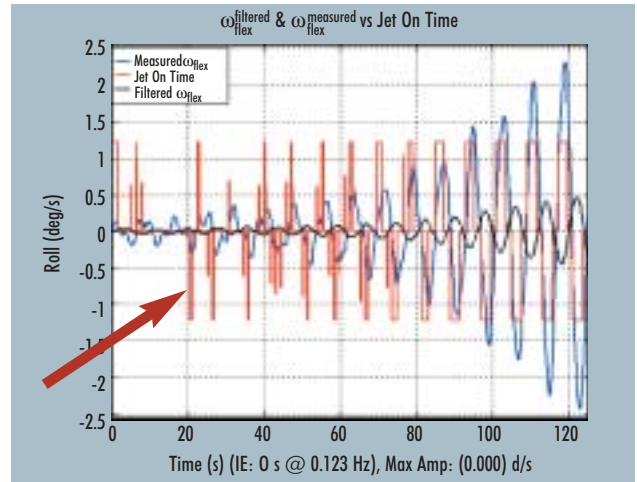
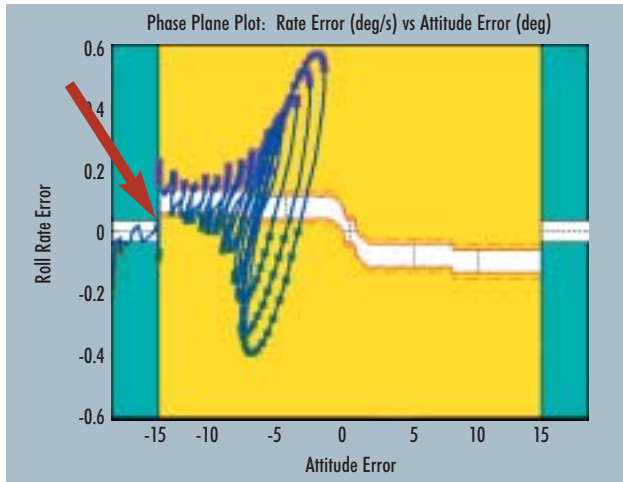


Figure 9. CSI Example: 18.65-deg maneuver angle - unstable ACS: phase plane, measured, and filtered flex vs jets (125 s and closeup), jet on-time, attitude, and fuel use.



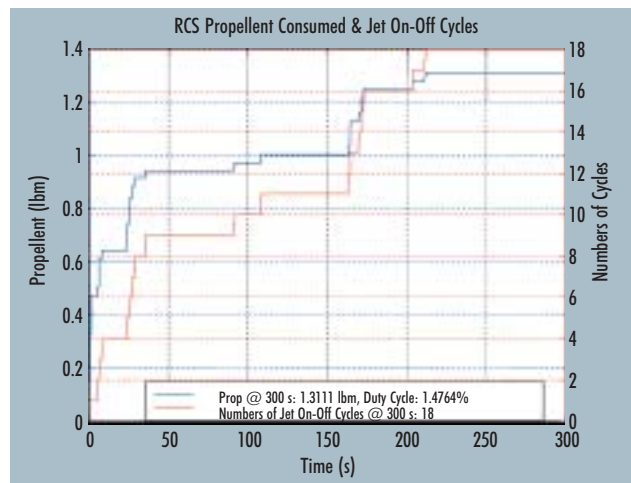
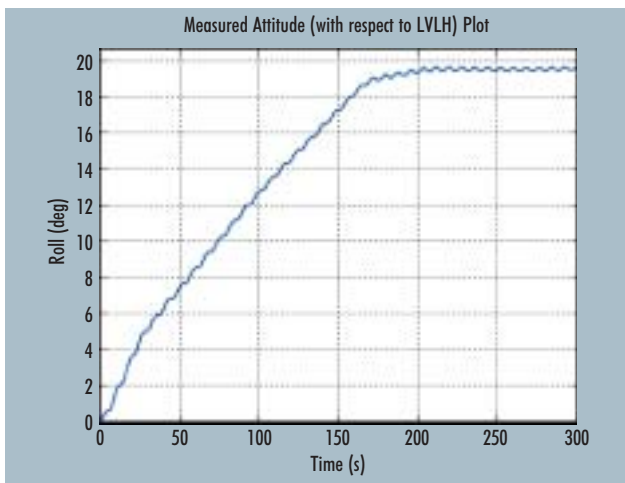
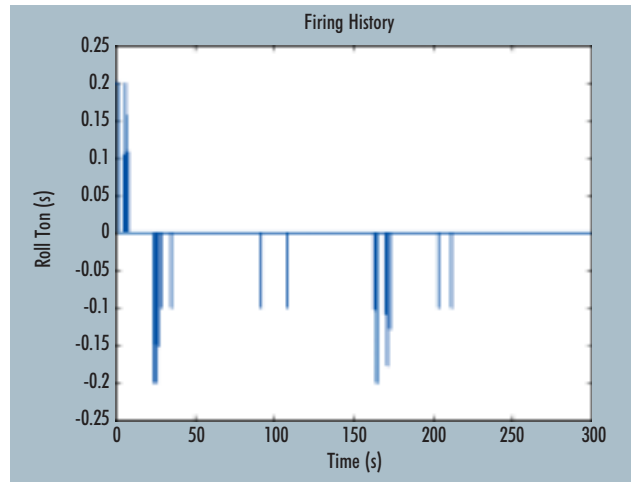
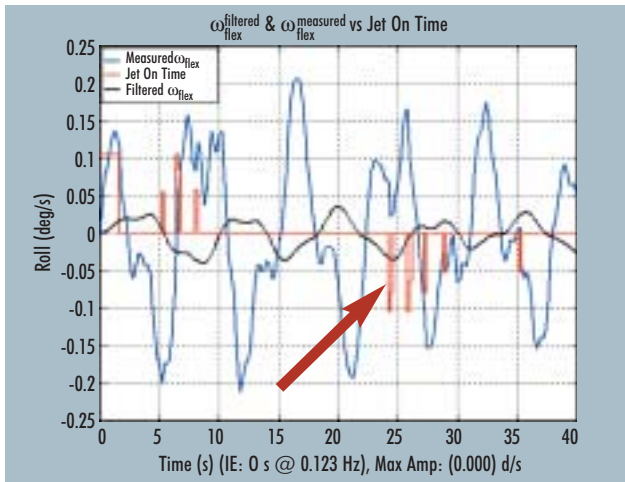
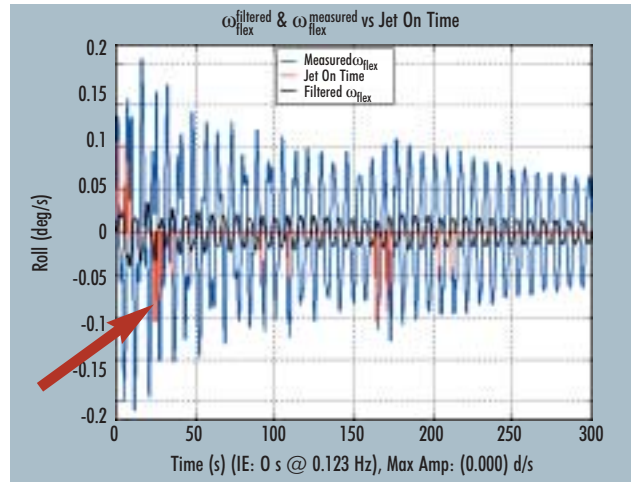
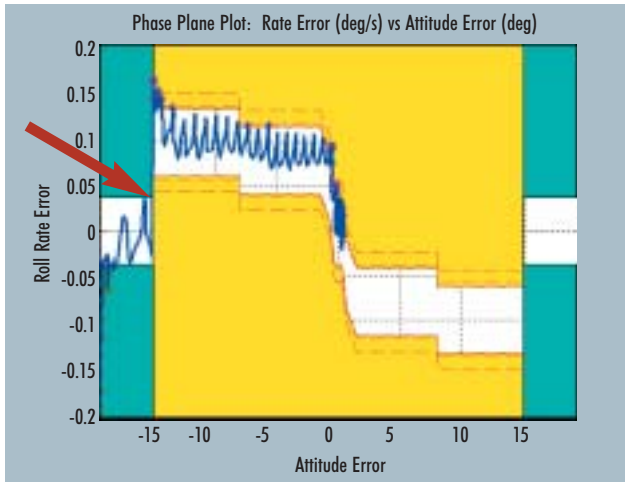


Figure 10. CSI example: 19.2-deg maneuver angle - stable ACS: phase plane, measured, and filtered flex vs jets (300 s and closeup), jet on-time, attitude, and fuel use.



individual firings are commanded based on current CMG momentum states until momentum reaches the desired levels. The pulse pattern can range from a single large pulse (Figure 11) to multiple high-frequency small pulses. An issue with such an approach is pulse phasing, which could coincide and excite a robotic structural mode and violate load limits. Also, this approach may take an unacceptably long time to complete. Another approach is to use nonperiodic, i.e., variable delay time, fixed-pulse-width firings (Figure 12), which also terminate when momentum reaches a prespecified value. A concern with such an approach is that loading frequency content varies with firing termination on a different pulse of a predefined pattern. This makes loads verification difficult. For these reasons, a feedback strategy was not considered.

For open-loop momentum desaturation, a predefined number of individual thruster firings are commanded at predetermined start times, while the CMGs are commanded in a feedforward manner to counter the thruster-induced momentum. The thruster pulse trains and CMG feedforward are designed to desaturate a specific amount of angular momentum. The pulse pattern can range from a single large pulse to multiple pulses with either periodic or nonperiodic delay times. A single large pulse is quick, efficient, and simple to implement. However, this method results in large induced loads. An alternative is to consider using a form of "command preshaping,"^{[3][4][5]} which effectively notches out the dominant resonant frequencies. However, since preshaping is a model-based approach, it requires knowledge of the structural modal frequencies. For flexible structures like the Station, the uncertainty and variability in mode frequencies makes it difficult to use such an approach.

Using multiple fixed pulse-width firings at periodic delay times between firings does reduce loads substantially, however, the phasing of the multiple firings remains an issue, as detailed in the previous section. This is the preferred strategy when structural characteristics are known. This type of pulsing strategy is currently being used by the Space Shuttle alternate primary reaction control system (PRCS) mode.^[2] Using multiple fixed pulse-width firings at nonperiodic delay times between firings resolves the phasing issue with periodic firings while at the same time reducing loads. This approach can be extended further by also considering nonperiodic thruster pulse-width firings. Hence, this desaturation strategy requires choosing delay times to robustly minimize loads. The advantages of such an approach are that the pulse pattern can be chosen early in the Space Station design phase and verified for all vehicles and operations. It also requires minimal ground support during flight and satisfies the issues associated with desaturation. Due to the desirable features of an open-loop approach to momentum damping, multiple fixed pulse-width firings at nonperiodic delay times were chosen as the architecture to robustly meet the design goals mentioned previously.

The design objective for the firing strategy is to minimize structural loads in the presence of plant uncertainty, such that a new pulse pattern is not required for every possible Space Station configuration. One approach is to implement a nonperiodic delay pulsing pattern where the delays are chosen randomly in order to avoid interaction with shifting and unknown resonances. This approach, however, is robust with respect to on-time, but not with respect to frequency. Our approach is to consider the frequency content or power spectral density (PSD) of the pulsing pattern and to choose the

delay time such that the flexible body mode excitation is minimized over a certain frequency range.^[6] This results in a pulsing strategy that is robust with respect to frequency (Figure 13). Hence, the optimization problem for a specified frequency range $[\omega_1, \omega_2]$ can be stated as^[6]

$$\min_{\tau_i} \max_{\omega \in [\omega_1, \omega_2]} \Phi_{uu}(\omega)$$

subject to

- (1) Fixed thruster on-time/pulse.
- (2) Fixed total delay time.
- (3) Fixed delay time range.

In the above, $\Phi_{uu}(\omega)$ is the PSD of the thruster pulse train. Note that since the PSD of the input signal is a function of the number and magnitude of delay time parameters, τ_i , it can be shaped by a judicious selection of the τ_i . Such a selection has the effect of maximizing the uniformity of the power in the chosen band and reducing the concentration of power at any one particular frequency.

For the ISS, CMG desaturation during robotic payload activity, a threshold of 10,000 ft-lb-s is used with a CMG feedforward torque of approximately 170 ft-lb, resulting in total desaturation time of approximately 1 min. Further, the thruster pulse widths were assumed to be 1.5 s based on a 5-pulse/4-delay pattern to reflect a worst-case scenario of a minimum of 1333 ft-lb thruster torque in a worst axis during assembly of the Station. This results in a 50-s constraint on the total allowable delay time. With regard to frequency, a range of 0.01 Hz to 1 Hz was used as a representative sample of expected Station/robotic structural modes. Solving for the optimal delay pattern using these constraints results in the delay and start times listed in Table 1. This CMG momentum desaturation method, developed by Draper Laboratory for the ISS, has been implemented in the Russian SM vehicle flight software.^[7]

Table 1. ISS CMG Momentum Desaturation Optimal Delays and Pulse Start Times.

Delay Number	1	2	3	4	
Optimal Delay (s)	17.3	10.9	8.4	13.4	
Pulse Number	1	2	3	4	5
Optimal Pulse Start Times (s)	0	18.8	31.2	41.1	56

CMG Attitude Control

Since the angular momentum of the CMG system is limited, manipulation of relatively heavy payloads may cause large momentum transients resulting in momentum and torque saturation. This situation is undesirable because it impacts the operational timeline of the assembly operation by requiring the use of the RCS to desaturate the CMGs, thus interrupting the payload operation. It is also undesirable because of the fuel use by the RCS and because of the structural load issues that arise by using the RCS while a massive payload is attached to one of the robotic arms.

CMG momentum use during the robotic operation depends on several factors. Clearly, it depends on the motion of the payload. The momentum use also depends on the commanded attitude of the Station during the payload operation. Since



external torques are being applied to the Station, the system angular momentum is not conserved. This means that the final CMG momentum depends on the path between the initial

and final attitudes, and not simply on the attitudes themselves. The initial and final attitudes are usually chosen to balance the external torques acting on the Station. Since the

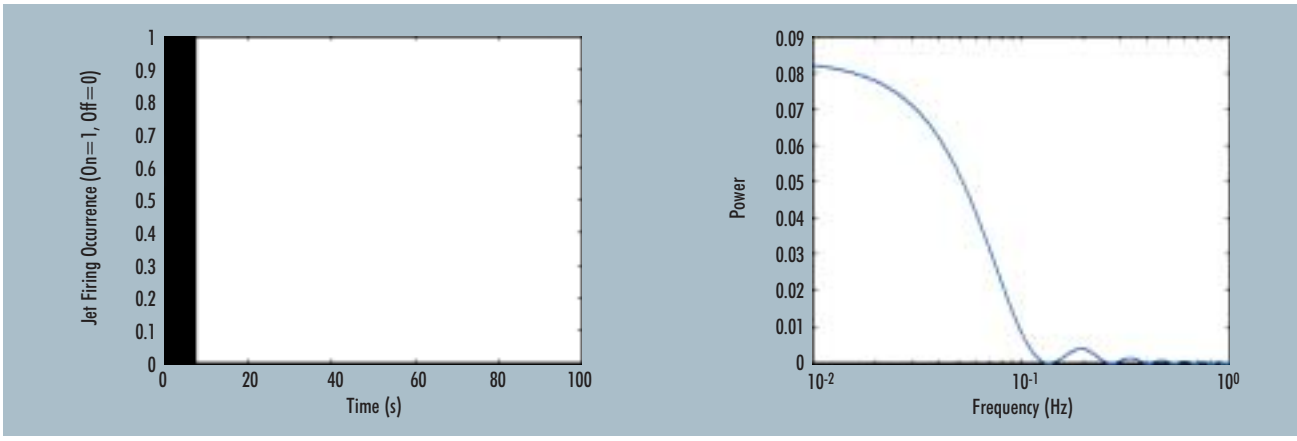


Figure 11. Single pulse in time and frequency (PSD) domain.

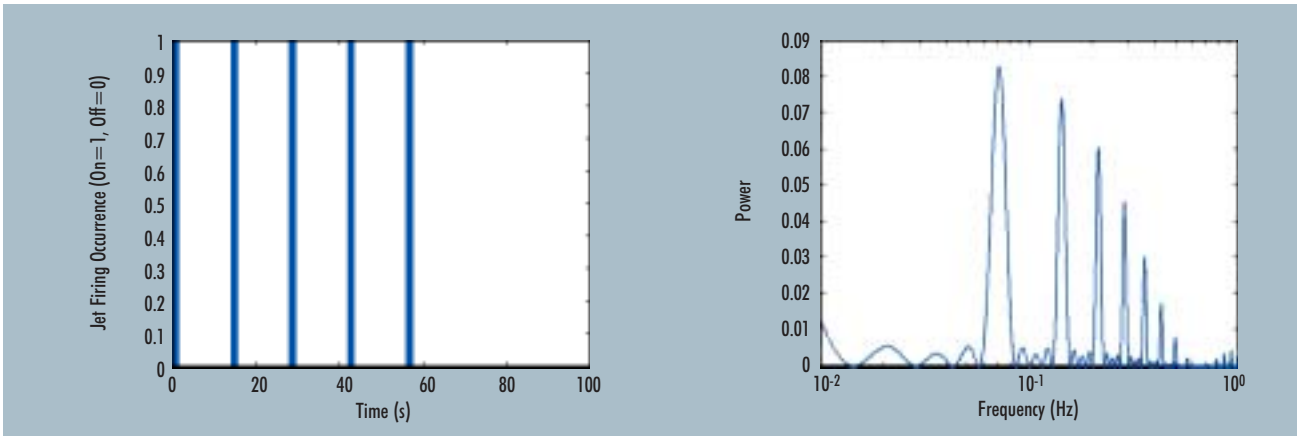


Figure 12. Fixed delay pulse in time and frequency (PSD) domain.

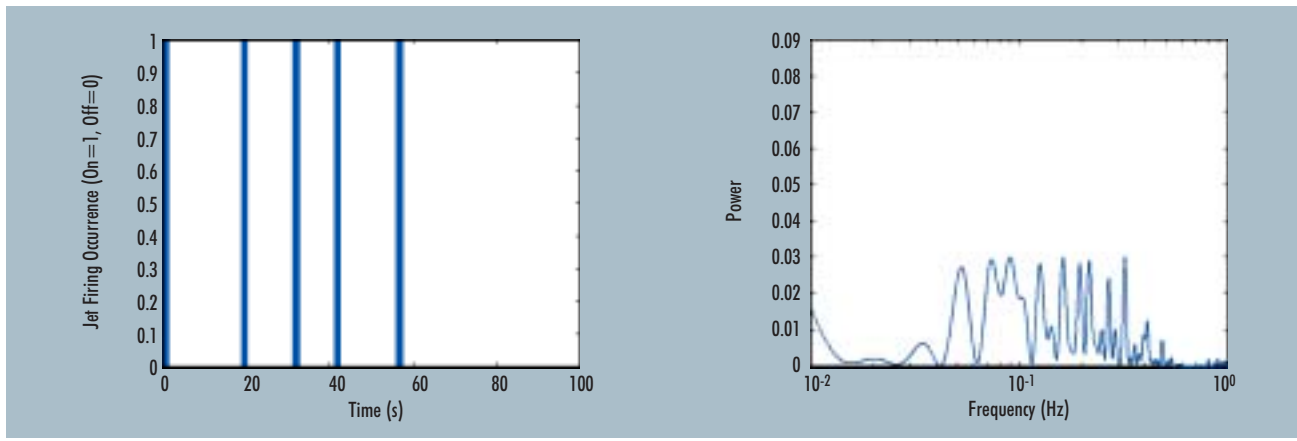


Figure 13. Power optimal pulse pattern in time and frequency (PSD) domain.



payload operation changes the mass properties of the Station, these equilibrium attitudes will also change. This requires an attitude maneuver to be performed during the payload operation. Some results on attitude maneuvers in the absence of external torques using momentum wheels and CMGs can be found in Refs. [8] and [9]. In Ref. [8], both open-loop and closed-loop optimal control strategies are considered. Since in general, Space Station angular momentum is not conserved due to the presence of gravity gradient and aerodynamic torques and the fact that payload motion complicates the vehicle dynamics motivates the analysis approach presented in the following.

Payload Dynamics Formulation

The payload dynamics formulation relies on efficiently modeling the dominant dynamics of a connected system of rigid bodies moving relative to each other by using appropriate simplifying assumptions. The standard rigid-body formulation of Station robotic operations include 6-degree-of-freedom (DOF) Shuttle/Station base body dynamics coupled to either a 6-DOF SRMS or 7-DOF SSRMS with attached payload. To reduce the dynamical complexity of the standard formulation, first, the robot arm dynamics are neglected, resulting in 6-DOF base body and 6-DOF payload dynamics. This is a reasonable assumption since the arm mass properties are much smaller than either the payload or the base body. To further simplify the dynamics, the payload motion kinematics are assumed to be prescribed, i.e., the robot joint controllers track the commanded arm trajectory with minimal error. This assumption eliminates the need to model the payload dynamics, and hence, reduces the problem to 6-DOF for the base or core body dynamics. Finally, by using relative (to base body) payload position and orientation parameters and a standard center of mass identity, the system angular momentum is decoupled from its linear momentum and is expressed compactly as

$$H_{\text{sys}} = D_0 \omega_{\text{ss}} + h_{\text{pld}} + h_{\text{cmg}}$$

where:

$$h_{\text{pld}} = D_{1a} \omega_{\text{pld/ss}} + D_{11} v_{\text{pld/ss}}$$

$$D_0 = I_{\text{ss}} + \mathfrak{R}_{\text{ss}}^{\text{pld}} I_{\text{pld}} \mathfrak{R}_{\text{ss}}^{\text{pld}\text{T}} - \frac{m_{\text{ss}} m_{\text{pld}}}{m_{\text{ss}} + m_{\text{pld}}} \begin{bmatrix} p_{\text{pld/ss}}^{\times} \\ p_{\text{pld/ss}}^{\times} \end{bmatrix}$$

$$D_{1a} = \mathfrak{R}_{\text{ss}}^{\text{pld}} I_{\text{pld}} \mathfrak{R}_{\text{ss}}^{\text{pld}\text{T}}$$

$$D_{11} = \frac{m_{\text{ss}} m_{\text{pld}}}{m_{\text{ss}} + m_{\text{pld}}} \begin{bmatrix} p_{\text{pld/ss}}^{\times} \\ p_{\text{pld/ss}}^{\times} \end{bmatrix}$$

In the above, all parameters are expressed in the core body or Space Station reference frame unless otherwise noted, h_{pld} represents the payload angular momentum relative to the core body, h_{cmg} represents the CMG angular momentum, $p_{\text{pld/ss}}$, $v_{\text{pld/ss}}$ represent the payload translational position and velocity relative to the Space Station, $\mathfrak{R}_{\text{ss}}^{\text{pld}}$, $\omega_{\text{pld/ss}}$ represent the payload angular orientation (rotation matrix) and velocity relative to the core body, and I_{pld} is the payload inertia expressed in the payload axis system.

With these simplifications, the system dynamics are reduced to a 3-DOF Newton-Euler type formulation^[10]

$$D_0 \dot{\omega} = -\dot{D}_0 \omega - \omega \times [D_0 \omega + h_{\text{pld}} + h_{\text{cmg}}] - \dot{h}_{\text{pld}} - \dot{h}_{\text{cmg}} + \tau_{\text{gg}} + \tau_{\text{aero}} \quad (1)$$

In the above, τ_{gg} and τ_{aero} represent the gravity gradient and aerodynamic torques on the Space Station. In this paper, aerodynamic torques are neglected for convenience. The corresponding attitude kinematics are obtained from standard quaternion formulation for angular velocity^[11]

$$\dot{\epsilon} = 0.5 \left(\epsilon^{\times} + \sqrt{1 - \epsilon^{\text{T}} \epsilon} 1_3 \right) (\omega - \omega_{\text{orb}}(\epsilon)) \quad (2)$$

where ϵ is the vector part of the quaternion representing the attitude of the Station body-fixed frame with respect to the rotating local vertical local horizontal (LVLH) reference frame, and ω_{orb} is the angular velocity inherent in maintaining attitude in the rotating LVLH reference frame. Augmenting the core body dynamics with the CMG momentum controller then forms the complete set of governing equations

$$\dot{h}_{\text{cmg}} = k_1 D_0 (\omega - \omega_{\text{orb}}(\epsilon_c)) + k_2 D_0 (\epsilon - \epsilon_c) \quad (3)$$

where k_1 and k_2 are the proportional and derivative gains of the CMG controller, and ϵ_c is the commanded attitude of the Station.

Attitude Control During Payload Operations

Maintaining CMG attitude control during robotic payload operations without exceeding the momentum limits requires a commanded attitude control strategy during the robotic operations. A standard approach is to command an instantaneous torque equilibrium attitude (TEA). A TEA is any constant spacecraft attitude with respect to a rotating reference frame that results in the sum of all external and gyroscopic torques being equal to zero.^[12] The benefits of such a strategy are that they are (locally) optimal solutions. Commanding an instantaneous TEA minimizes the external disturbance torques on the vehicle. However, in cases where the TEA is not constant due to payload motion, following such a strategy does not account for the cost (in momentum) of following the TEA trajectory. It also does not anticipate the change in TEA due to payload motion. Since the payload trajectory is assumed known in advance, this information could be used in generating momentum-minimizing attitude command schedules.

From an operational standpoint, it would be desirable to avoid saturating the CMGs during payload motion. In general, to minimize CMG momentum use for attitude hold prior to and after the payload operation, it is envisioned that the local TEA attitude would be commanded. Hence, an optimization problem can be defined to minimize peak momentum magnitude by an appropriate choice of attitude command during the payload operation, i.e.

$$\min_{\epsilon_c} \left\| h_{\text{cmg}}^{\text{T}}(t) h_{\text{cmg}}(t) \right\|_{\infty} \quad (4)$$

subject to the Space Station dynamic Eqs. (1) and (2), the CMG control law, Eq. (3), and the following boundary conditions

$$\begin{aligned} \epsilon(0) &= \epsilon_0 & \epsilon(t_f) &= \epsilon_{t_f} \\ \omega(0) &= \omega_{\text{orb}}(\epsilon_0) & \omega(t_f) &= \omega_{\text{orb}}(\epsilon_{t_f}) \end{aligned} \quad (4a)$$

where ϵ_0 and ϵ_{t_f} are the initial and final TEA attitudes.



To solve this problem, an approach based on converting this problem to a nonlinear constrained function optimization approach was considered.^[10] Briefly stated, this approach first removes the dependency on commanded attitude as it simplifies the constraint dynamics and results in the optimization being a function of the Station attitude. Once the optimum (or any) attitude trajectory, $\epsilon(t)$, and its corresponding CMG momentum, $h_{cmg}(t)$, have been obtained, the corresponding attitude command $\epsilon_c(t)$ can be obtained by solving the CMG control law Eq. (3) for ϵ_c . The next step was to convert the optimal control problem to a function optimization problem, which in many cases is much simpler to solve. The conversion was accomplished by removing the derivative dependence from the constraints, which results in a nonlinear algebraic dependence of h_{cmg} on ϵ using finite difference approximations. At this stage, standard function optimization results can be applied. However, the mini-max criterion, Eq. (4), is not amenable to analytic solutions due to the lack of differentiability. However, Eq. (4) can be upper bounded by^[10]

$$\min_{\epsilon} \left\| h_{cmg}^T(t) h_{cmg}(t) \right\|_2 \quad (5)$$

Using the reformulated cost function, Eq. (5), the optimization problem can be solved either using standard Lagrange multiplier techniques for the constraints, or alternatively, the boundary conditions can be treated as known constants and eliminated from the optimization problem.

Simulation Results

The methodology developed in Ref. [10] was applied to the ISS robotic assembly for Stage 12A. The payload consists of the inboard port integrated truss segment P3/4, which is initially unberthed from the Shuttle payload bay by the SRMS, then handed off to the SSRMS for installation on the Station as shown in Figure 14. The vehicle principal axes corresponding to the preplanned payload trajectory are shown in Figure 15. The CMG momentum use for various attitude command strategies during robotic payload assembly operation is shown in Figure 16.

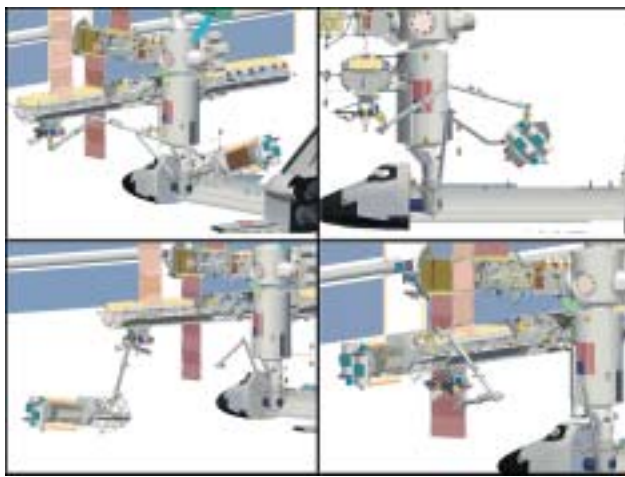


Figure 14. ISS Stage 12A robotic payload assembly operation.

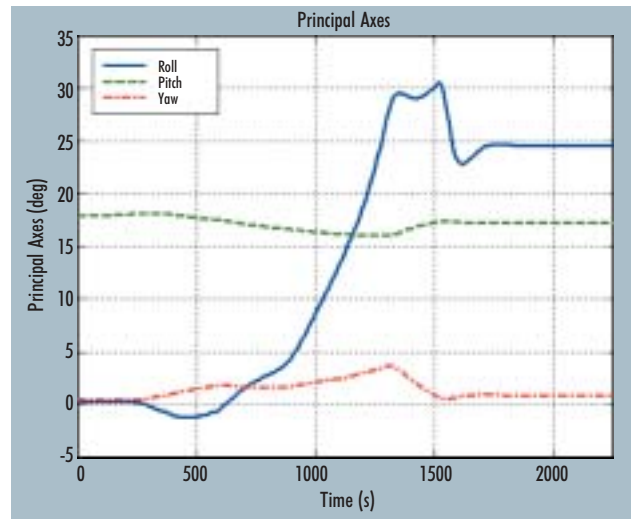


Figure 15. ISS Stage 12A principal axes during robotic payload assembly operation.

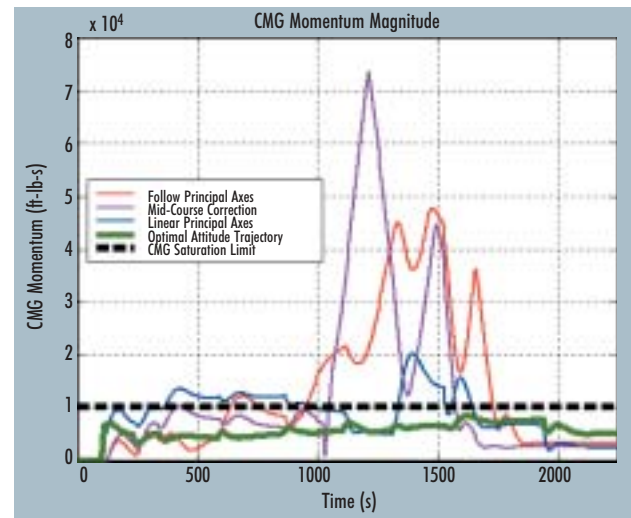


Figure 16. ISS Stage 12A CMG momentum use for various attitude command strategies during robotic payload assembly operation.

Table 2. ISS Stage 12A CMG Peak Momentum Use for Various Strategies.

Test Cases	CMG Momentum [ft-lb-s]	
	Peak 2-norm	Final 2-norm
Follow Principal Axes	47,696	3,251
Mid-Course Correction	73,513	2,565
Linear Principal Axes	20,256	2,376
Optimal Attitude Trajectory	8,396	5,194



The optimal attitude command trajectories were compared to three other alternative strategies.^[10] In the following, the notation TEA is equivalent to principal axes:

- Follow Principal Axes: Command instantaneous TEA.
- Mid-Course Correction: Command initial TEA for the first half of the maneuver, then command final TEA for the second half of the maneuver.
- Linear Principal Axes: Command a linear interpolation between the initial TEA and final TEA.
- Optimal Attitude Trajectory: Command momentum optimal attitude.

The time step for all test cases is 10 s. The peak and final CMG momentum magnitudes for all four test cases are summarized in Table 2. It is evident that the optimal attitude trajectory results in the best CMG momentum performance and, theoretically, does not require momentum desaturation. The optimal attitude command trajectory results are shown in Figure 17. Using this attitude history as the CMG attitude command resulted in reducing the peak CMG momentum to 8,400 ft-lb-s, which is below the momentum desaturation limit. One interesting characteristic of this trajectory is the jump in CMG momentum at the beginning and end of the maneuver. This is similar in nature to the bang-coast-bang fuel optimal solution for a maneuver.

Conclusions

This paper reviewed control challenges related to the assembly and operation of the International Space Station. Changing Station characteristics during assembly, such as variability in structural flexibility and mass properties, were identified as issues that must be addressed for a successful Station program. Three examples of control challenges were reviewed in this paper; the first two arise out of variability in flex structure, and the last one is due to mass property variation. Controller/flex structure interaction issues and their origins were reviewed, as well as representative examples for a particular assembly stage. CMG momentum desaturation issues during robotic operations were addressed, and an operational solution was reviewed. Finally, CMG attitude control issues during payload robotic operations were presented, as well as an issue resolution technique.

Acknowledgments

The author would like to acknowledge the assistance of Edward McCants and Dr. Jian-Woei Jang, who contributed to the work documented here and to the preparation of this paper. The work documented in this paper was completed under NASA Contract NAS9-1556.

References

- [1] Hall, R., K. Kirchwey, M. Martin, G. Rosch, D. Zimpfer, "Flight Control Overview of STS-88, The First Space Station Assembly Flight," *Proc. 1999 AAS/AIAA Astrodynamics Conference*, AAS Paper No. 99-371, August 1999.
- [2] Zimpfer, D., K. Kirchwey, D. Hanson, M. Jackson, and N. Smith, "Shuttle Stability and Control of the STS-71 Shuttle/MIR Mated Configuration," *Proc. 1996 AAS/AIAA Spaceflight Mechanics Conference*, AAS Paper No. 96-131, February 1996.
- [3] Meckl, P.H. and W.P. Seering, "Minimizing Residual Vibration for Point-to-Point Motion," *Journal of Vibration, Acoustics, Stress and Reliability in Design*, Vol. 107, October 1985, pp. 378-382.
- [4] Seering, W.P. and N.C. Singer, "Using Acausal Shaping Techniques to Reduce Robot Vibration," *Proc. 1988 IEEE International Conference on Robotics and Automation*, April 1988, pp. 1434-1437.
- [5] Wie, B., *Space Vehicle Dynamics and Control*, AIAA Education Series, 1998, pp. 623-626.
- [6] Bedrossian, N., J. Lepanto, N. Adams, J. Sunkel, and T. Hua, "Jet Firing Strategy to Minimize Structural Loads," *Proc. 1995 American Control Conference*, June 1995, pp. 3622-3626.
- [7] Bedrossian, N., "International Space Station CMG Momentum Desaturation Design," *Proc. 2000 AIAA Guidance, Navigation, and Control Conference*, Paper No. AIAA-2000-4452, August 2000.
- [8] Vadali, S.R. and J.L. Junkins, "Optimal Open-Loop and Stable Feedback Control of Rigid Spacecraft Attitude Maneuvers," *Journal of the Astronautical Sciences*, Vol. 32, No. 2, 1984, pp. 105-122.
- [9] Carrington, C.K. and J.L. Junkins, "Spacecraft Attitude Control Using Generalized Angular Momenta," *Proc. AIAA/AAS Astrodynamics Conference*, AAS Paper No. 85-361, August 1985.
- [10] Bedrossian, N. and E. McCants, "Space Station Attitude Control During Payload Operations," *Proc. 1999 AAS/AIAA Astrodynamics Conference*, AAS Paper No. 99-372, August 1999.
- [11] Hughes, P.C., *Spacecraft Attitude Dynamics*, J. Wiley & Sons, 1986, p. 26.
- [12] Elgersma, M.R. and D.S. Chang, "Determination of Torque Equilibrium Attitude for Orbiting Space Station," *Proc. 1992 AIAA Guidance, Navigation and Control Conference*, AIAA Paper No. 92-4481, August 1992, pp. 924-931.

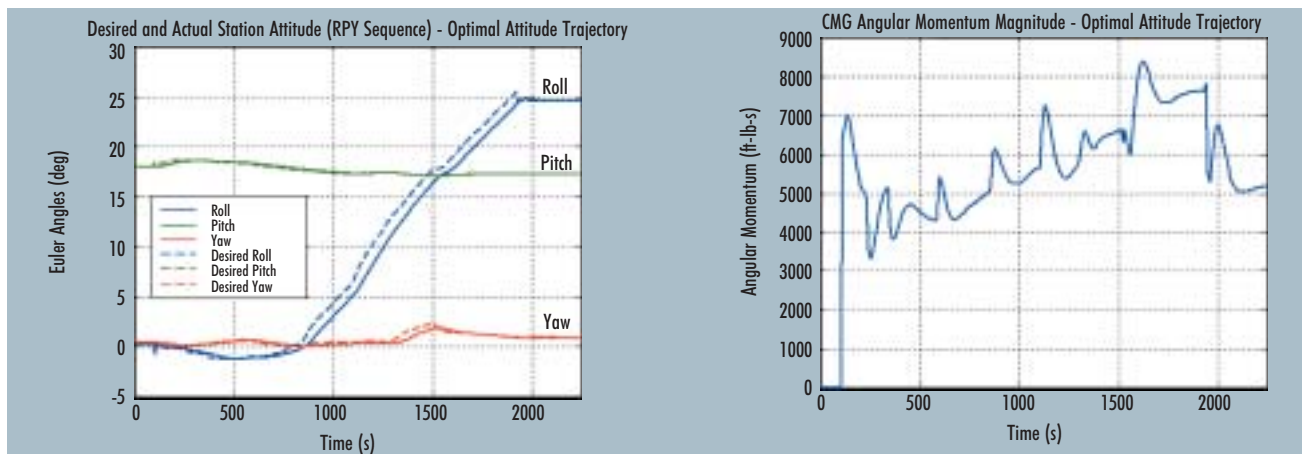
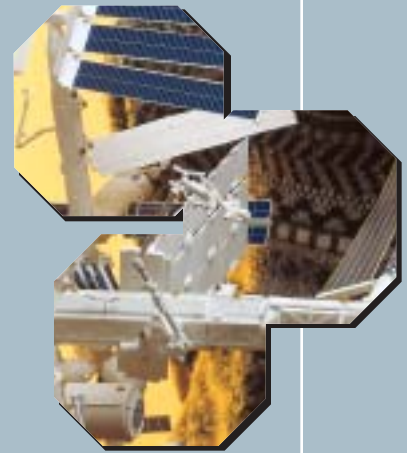


Figure 17. Optimal attitude trajectory results: commanded and actual Euler angles (RPY sequence) and CMG momentum magnitude.





Nazareth S. Bedrossian



Biography



Nazareth S. Bedrossian

bedrossian@draper.com

is a Principal Member of the Technical Staff and the Task Leader for the International Space Station (ISS) Dynamic Interaction Task. He designed the ISS momentum desaturation algorithm now used in the flight software. He also represents NASA Johnson Space Center as technical point of contact for Russian ISS attitude control systems. Dr. Bedrossian originated and leads the development of the eSim project (<http://www.jsc.draper.com/esim/>), a Web-enabled distributed analysis and simulation platform. He established and directs the Draper Graduate Fellowship program at Rice University. Recently, he expanded the Fellow program to include graduates of the U.S. Air Force Academy. From 1997-1999, he was Associate Director of the Instrument Society of America (ISA) Robotics Division. In 1999, he organized and chaired the AIAA/NASA/ISA Workshop on Robotics MEMS. He serves on the steering committee for the NASA Aerospace Technology Working Group. He is the author of 21 conference and journal articles on the kinematics, dynamics, and control of spacecraft and robotic systems. Dr. Bedrossian received a BS in Mechanical Engineering from the University of Florida and SM and PhD degrees from MIT as a Draper Fellow, all in Mechanical Engineering.

